International Journal of Data and Network Science 8 (2024) 989–1000

Contents lists available at GrowingScience

International Journal of Data and Network Science

homepage: www.GrowingScience.com/ijds

A novel four-wing chaotic system with multiple equilibriums: Dynamical analysis, multistability, circuit simulation and pseudo random number generator (PRNG) based on the voice encryption

Khaled Benkouider[a], Issam A.R. Moghrabi[b], Aceng Sambas[c,d], Sezgin Kaçar[e], Süleyman Uzun[f], Basim A. Hassan[g], Ibrahim Mohammed Sulaiman[h,i], Sundarapandian Vaidyanathan[j] and Mohamad Afendee Mohamed[b] and Jumadil Saputra[k*]

[a]*Non Destructive Testing Laboratory, Automatic Department, Jijel University, BP.98, 18000, Jijel, Algeria*
[b]*Computer Science Department, School of Arts and Sciences, University of Central Asia, Naryn, Kyrg. Republic*
[c]*Faculty of Informatics and Computing, Universiti Sultan Zainal Abidin, Gong Badak, Kuala Terengganu 21300, Malaysia*
[d]*Department of Mechanical Engineering, Universitas Muhammadiyah Tasikmalaya, Tasikmalaya, West Java 46196, Indonesia*
[e]*Department of Electrical and Electronics Engineering, Sakarya University of Applied Sciences, Sakarya, 54050, Türkiye*
[f]*Department of Computer Engineering, Sakarya University of Applied Sciences, Sakarya, 54050, Türkiye*
[g]*College of Computer Science and Mathematics, University of Mosul, Iraq*
[h]*School of Quantitative Sciences, College of Art and Sciences, Universiti Utara Malaysia, Sintok, 06010, Kedah, Malaysia*
[i]*Faculty of Education and Arts, Sohar University, Sohar 311, Oman*
[j]*Centre for Control Systems, Vel Tech University, Vel Nagar, Avadi, Chennai 600 062, Tamil Nadu, India*
[k]*Universiti Malaysia Terengganu, 21030 Kuala Nerus, Terengganu, Malaysia*

C H R O N I C L E

Article history:
Received: November 10, 2023
Received in revised format: November 20, 2023
Accepted: December 8, 2023
Available online: December 8, 2023

Keywords:
Chaotic systems
Circuit
Multi-stability
PRNG
Voice encryption

A B S T R A C T

Recently, there has been tremendous interest worldwide in the possibility of using chaos in communication systems. Many different chaos-based secure communication schemes have been proposed up until now. However, systems with strong chaoticity are more suitable for chaos-based secure communication. From the viewpoint of Lyapunov exponents, a chaotic system with a larger positive Lyapunov exponent is said to be more complex. This paper constructing a multistable chaotic system that can produce coexisting attractors is an attractive field of research due to its theoretical and practical usefulness. An innovative 3D dynamical system is presented in this research. It can display various coexisting attractors for the same values of parameters. The new system is more suitable for chaos-based applications than recently reported systems since it exhibits strong multistable chaotic behavior, as proved by its large positive Lyapunov exponent. Furthermore, the accuracy of the numerical calculation and the system's physical implementations are confirmed by analog circuit simulation. Finally, implementing the proposed voice encryption is done using a four-wing chaotic system based on the PRNG.

1. Introduction

Recently, there has been tremendous interest worldwide in the possibility of using chaos in communication systems. Many different chaos-based secure communication schemes have been proposed up until now (Rahman & Jasim, 2022; Ilyas et al., 2022). For that reason, many chaotic systems have been constructed and reported in the literature (Gao et al., 2023; Zhao et al., 2023). However, systems with strong chaoticity are more suitable for chaos-based secure communication. From the viewpoint of Lyapunov exponents, a chaotic system with a larger positive Lyapunov exponent is said to be more complex. On the

* Corresponding author.
E-mail address: jumadil.saputra@umt.edu.my (J. Saputra)

ISSN 2561-8156 (Online) - ISSN 2561-8148 (Print)

doi: 10.5267/j.ijdns.2023.12.008

other hand, the multistability phenomenon in some chaotic systems can be very useful because it makes the system more complex and mapped to the possible construction of more secure applications. The multistability phenomenon signals the generation of coexistence of different chaotic attractors as a function of only its initial condition. Numerous studies have been conducted on chaotic systems with multistability and coexisting attractors (Sambas et al., 2022; Faradja & Qi, 2020).

Recently, many different chaotic systems have been constructed starting from the number wing of attractors, such as one-wing attractors (Zhang et al., 2018), double-wing attractors (Sambas et al., 2019), three-wing attractors (Zhou et al., 2017), four-wing attractors (Deng et al., 2020), and multi-wing attractors (Cui et al., 2020) . Many different voice encryption applications have used the principle of chaos systems, such as the construction of a random number generator (RNG) for the development of a novel voice encryption algorithm that was reported in (Mobayen et al., 2020). Sadkhan and Mohammed (2015) proposed a random unified chaotic map as a pseudo-random bit generator (PRBG) and its application in digital voice encryption based on wireless communication. Rajagopal et al. (2019) modified the conventional Chua's circuit with a non-ideal voltage-controlled memristor with a quadratic internal state and implemented MMCC for voice encryption. García-Sepúlveda et al. (2020) studied modulated chaotic signals to improve the encryption quality by shifting the energy to the encrypted frequency band. An example of speech encryption using a 4-D blinking chaotic system is shown by Elsadany et al. (2023), with encryption keystream dynamically generated using pre-treated chaotic mixed sequences. Alemami et al. (2020) proposed a secured speech recording via multiple encryption algorithms constructed based on chaotic logistic and sine maps. Li et al. (2014) introduced a voice encryption algorithm using compound chaotic mapping that achieved high security. Al-Hazaimeh (2019) proposed a dynamic speech encryption algorithm based on Lorenz chaotic map over internet protocol to increase the service performance of the real-time applications. Another audio encryption algorithm due to Farsana and Gopakumar (2016) was introduced by combining the principle of permutation and substitution (with keystream) of sampled audio using respective discrete modified Henon map and the modified Lorenz - Hyperchaotic system.

Meanwhile, Hasan et al. (2022) proposed a digital speech cryptography algorithm that encrypts the converted voice file using random keys generated by Hénon and Gingerbread chaotic maps. Al-Hazaimeh et al. (2022) proposed another Jacobian elliptic map-based speech encryption scheme with sufficiently large key space for a better security level. Akmeşe et al. (2023) studied random number generation and sound encryption applications with a Langford fractional chaotic system. Also, this research can be used in cryptology, secret writing, stamping, statistical sampling, computer simulations, dynamic information compression, and coding. However, discussion about pseudo-random number generators (PRNG) based on voice encryption is still problematic in the chaotic system.

This paper contributes to (i) the system consists of nine terms, including three quadratics nonlinear terms, and the system exhibits hidden attractors. (ii) the system has a larger maximum Lyapunov exponent compared with the other similar system. (iii) the system exhibits coexisting attractors and multistability behavior, and (iv) the PRNG-based image encryption has been developed and applied for encryption

This paper initially introduced a novel 3D chaotic system with nine terms and five equilibrium points. The new dynamical system has rich behaviors such as periodic, chaotic, coexisting periodic behaviors and coexisting chaotic behaviors. The dynamical properties of the new model are discussed theoretically and numerically, including Lyapunov exponents, dissipativity, stability, bifurcation, and multistability. In addition, a comparative study is presented, which shows that our system is much stronger than other literature. Using Multisim software, an equivalent electronic circuit schematic diagram is designed, validating the theoretical study and demonstrating the physical feasibility of the new mathematical 3D model. Finally, implementing the proposed voice encryption is done using a four-wing chaotic system based on the PRNG.

2 Mathematical Model of the Proposed Four-Wing System

In Eq. (1), we can identify the proposed dynamical systems with the novel four-wing chaotic behavior.

$$\begin{cases} \dot{x} = a(y - x) + yz \\ \dot{y} = bx + cy - xz \\ \dot{z} = -dz + xy + 1 \end{cases} \tag{1}$$

with x, y, and z being the state variables and a, b, c, and d being the control parameters.

This proposed system (system (1)) exhibits the properties of chaoticity if we choose the initial state, $[x_0, y_0, z_0] = [0.5, 0.2, 0.5]^T$ and [a, b, c, d] = [10, -5, 10, 30]. To be more precise, for these parameter values, the proposed system generates four-wing chaotic attractors, as shown in Fig. 1.

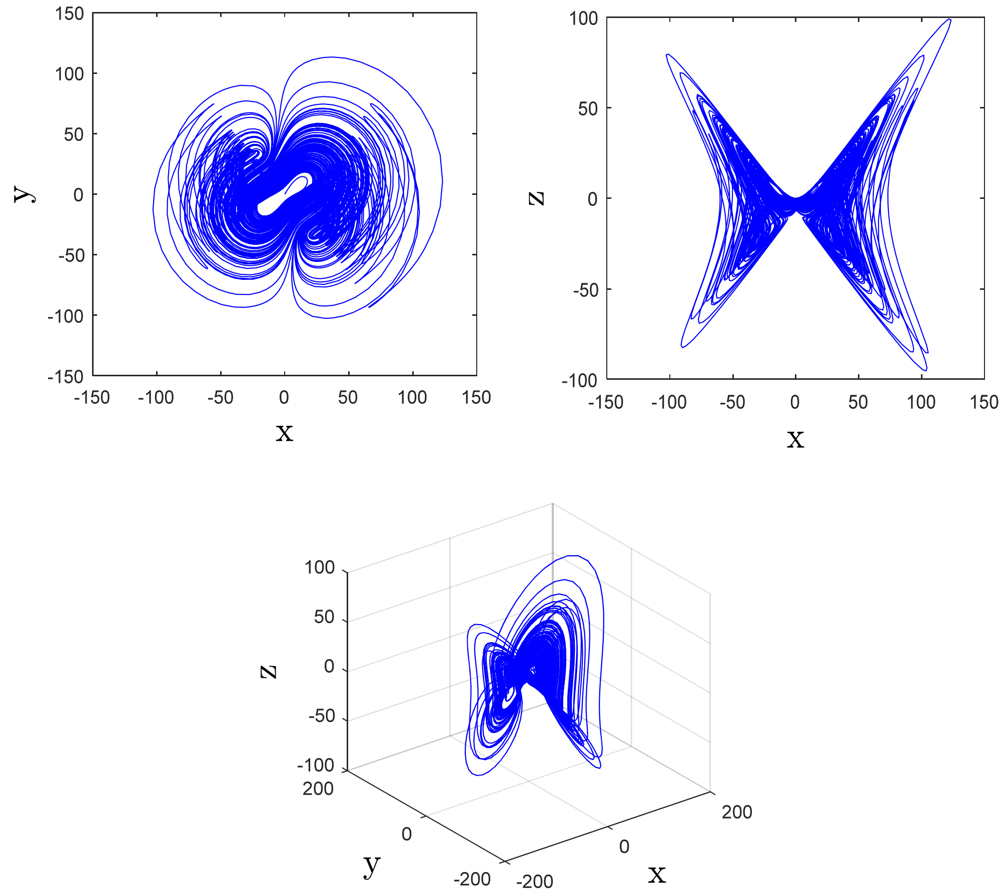

Fig. 1. Four-wing chaotic attractors for the proposed chaotic system

Using the values of system's parameters, we can calculate the respective Lyapunov exponents using Wolf's algorithm incorporated on MATLAB as:

$$\begin{cases} LE_1 = 2.993 \\ LE_2 = 0 \\ LE_3 = -32.992 \end{cases} \quad (2)$$

From Eq. (2), we calculated the sum of Lyapunov exponents to be negative, and thus confirming the dissipative properties belong to the proposed chaotic system. In general, a system's sensitivity to initial values determines the characteristics of a chaotic system by which the highly sensitive system is known to possess stronger chaos. Fig. 2 exhibits an extremely different evolution of the first state coordinate of the proposed chaotic system for two very close initial conditions.

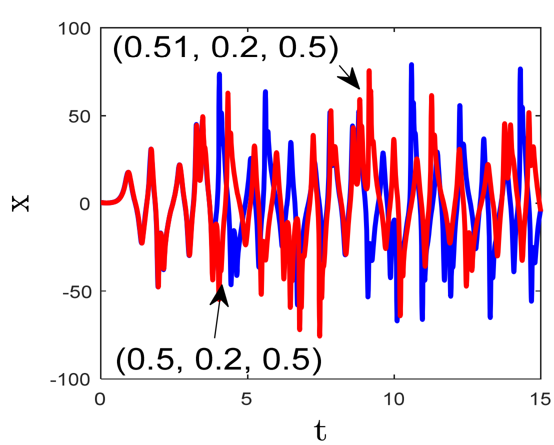

Fig. 2. Time series of the x variable for $x_0 = 0.5$ (in blue) and $x_0 = 0.51$ (in red)

Table 1 compares the maximum Lyapunov exponents (MLE) of the proposed chaotic system against that of other literature. Our system showed that it is much stronger than other reported systems. Such property is found to be more recommendable for the development of chaos-based applications.

Table 1
Comparison of Maximum Lyapunov Exponents with other literature

3D Chaotic System	MLE
Lu et al. (2002)	1.504
Liu et al. (2004)	1.643
Cai & Tan (2007)	2.395
Munmuangsaen & Srisuchinwong (2009)	1.491
Chen et al. (2008)	1.400
Vaidyanathan (2016)	1.501
Benkouider et al. (2021)	1.051
Proposed System	**2.993**

When we choose parameters as a = 30, b = 35, and c = 9, the proposed chaotic system has five equilibrium points:

$$\begin{aligned} E_1 &= [0,\ 0,\ 1/30] \\ E_2 &= [-10.32,\ -8.06,\ 2.81] \\ E_3 &= [10.32,\ 8.06,\ 2.81] \\ E_4 &= [-20.44,\ 91.99,\ 74.18] \\ E_5 &= [20.44,\ -91.99,\ 74.18] \end{aligned} \tag{3}$$

The stability perspective of the proposed chaotic system around these five equilibrium points was studied by examining the eigenvalues of the Jacobian matrix J_{E_i} , and the results are listed in Table 2.

Table 2
Stability inquiry into the proposed four-wing chaotic system

E_i	J_{Ei} eigenvalues	Stability
E_1	λ_1 = -30, λ_2 = -7.0355, λ_3 = 7.0355	Unstable
$E_{2,3}$	λ_1 = -32.0435, $\lambda_{2,3}$ = 1.0217±10.2981i	Unstable
$E_{3,4}$	λ_1 = -46.1566, $\lambda_{2,3}$ = 8.07829±20.3199i	Unstable

3 Dynamical Study of the Proposed Four-Wing Chaotic System

3.1 Bifurcation diagram and Lyapunov Exponents

The dynamical characteristics of the proposed 3D chaotic system versus the control parameter b are explored in this part by utilizing the Lyapunov exponents spectrum, bifurcation diagram, and phase plots. By allowing the control parameter b to be varied within the range [-5, 5] while fixing a = 10, c = 10, and d = 30, the respective plots for the Lyapunov exponents are spectrum and bifurcation diagram of this proposed system (refer to Fig. 3 (a) and Fig. 3(b)). When -5 < b < 3.8, it is observable from Fig. 3(b) that the proposed chaotic system has one positive Lyapunov exponent, which marks the chaotic behavior shown in Fig. 3(a). Specifically, when b = -2, the y-z chaotic attractor is plotted as in Fig. 4(a).

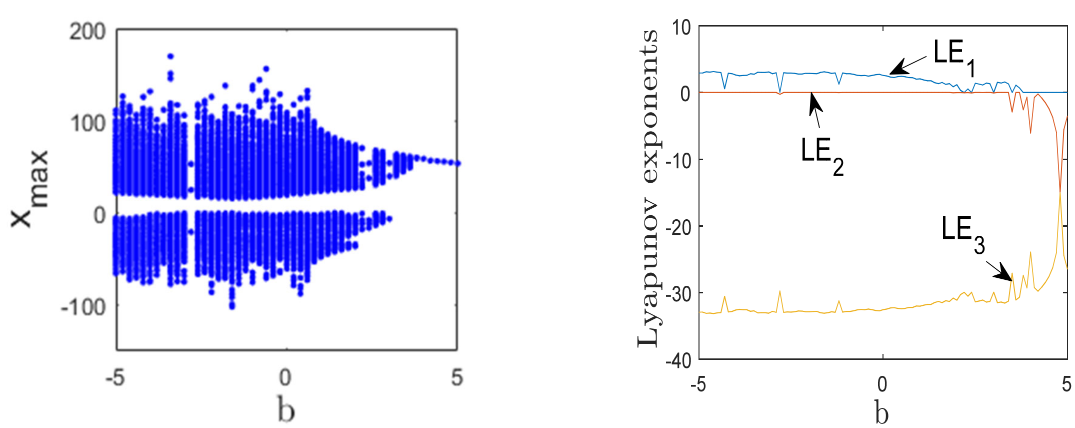

Fig. 3. Bifurcation diagram and LEs spectrum of the proposed chaotic system versus parameter b

The corresponding LEs are: $LE_1 = 2.863$, $LE_2 = 0$, $LE_3 = -32.865$. When $3.8 < b < 35$, it is observable from Fig. 3(b) that the proposed chaotic system has one zero and two negative Lyapunov exponents, which means that it exhibits periodic behavior as shown in Fig. 3(a). When $b = 5$, the *y-z* periodic attractor is plotted in Fig. 4(b). The corresponding LEs are: $LE_1 = 0$, $LE_2 = -3.479$, $LE_3 = -26.865$. Finally, it should be noted that there are some tiny windows of periodic behavior sandwiches between chaos when $b = -2.8$, $b = 3$, and $b = 3.5$.

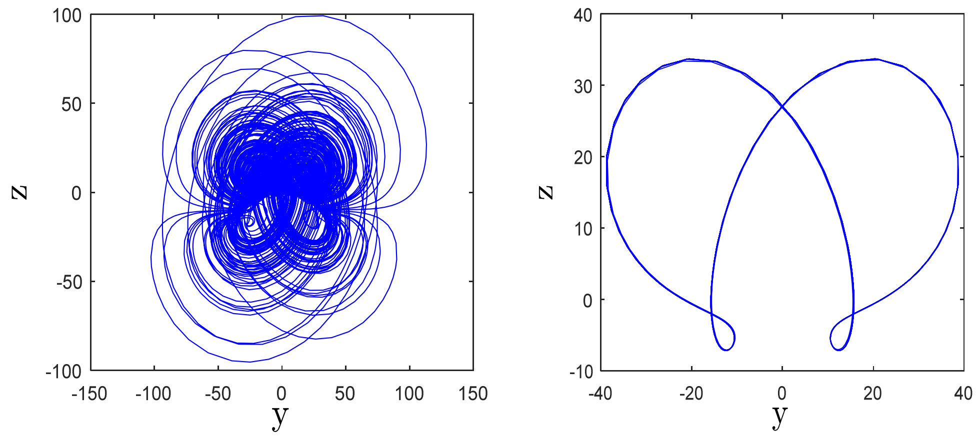

Fig. 4. Phase plots from the proposed chaotic system or specific values of parameter b

3.2. Multistability

The proposed chaotic system exhibits the coexistence of two periodic attractors or two chaotic attractors for different choices of parameter values. Let $I_{01} = (0.5, 0.2, 0.5)$ and $I_{02} = (-0.5, -0.2, 0.5)$ be two other initial points for the proposed 3D chaotic system, where we represent the state orbit corresponding to I_{01} as a blue color orbit and the state orbit corresponding to I_{02} as a red color orbit.

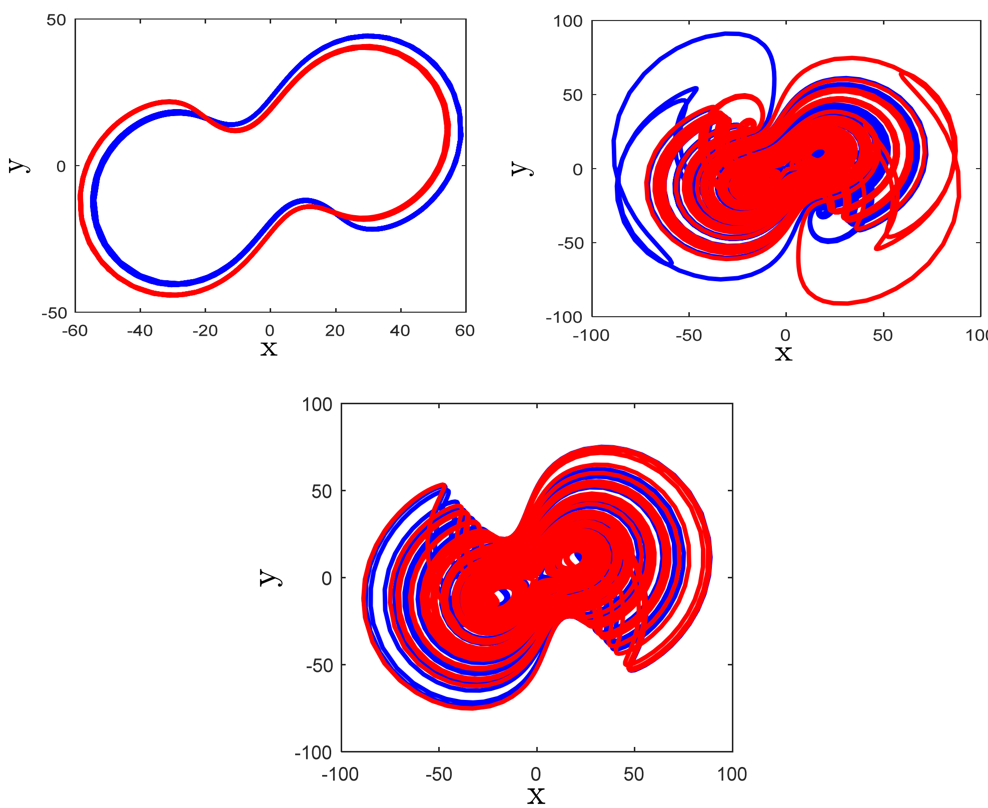

Fig. 5. The coexisting attractors generated by the proposed 3D chaotic system

By choosing different set of values for control parameters such as [$a = 10$, $b = 4$, $c = 10$, $d = 30$], [$a = 10$, $b = 1$, $c = 10$, $d = 30$], [$a = 10$, $b = -1$, $c = 10$, $d = 30$], the proposed chaotic system exhibits two coexisting chaotic attractors as shown in Fig.

5(a), Fig. 5(b), and Fig. 5(c) respectively

4. Circuit Design of the Novel Four-Wing Chaotic System

The analog circuit design for the proposed system can be found in Fig. 6. It was implemented using MULTISIM by combining components such as capacitors, resistors, operational amplifiers TL082CD and analog multipliers AD633JN. In fact, the circuit diagram in Fig. 6 can be converted into the respective circuital equations by employing Kirchhoff's laws to the proposed system to produce the following:

$$\begin{cases} \dot{x} = -\dfrac{1}{R_1C_1}x + \dfrac{1}{R_2C_1}y + \dfrac{1}{R_3C_1}yz \\ \dot{y} = -\dfrac{1}{R_4C_2}x + \dfrac{1}{R_5C_2}y - \dfrac{1}{R_6C_2}xz \\ \dot{z} = -\dfrac{1}{R_7C_3}z + \dfrac{1}{R_8C_3}xy - \dfrac{1}{R_9C_3}V_1 \end{cases} \tag{4}$$

where

$$\begin{cases} C_1 = C_2 = C_3 = 1nF \\ R_1 = R_2 = R_5 = 40k\,\Omega \\ R_3 = R_6 = R_8 = R_9 = 400k\,\Omega \\ R_4 = 80k\,\Omega \\ R_7 = 13.34k\,\Omega \\ R_i = 100k\,\Omega,\ \ i = 10,11,......,15 \end{cases} \tag{5}$$

The MultiSim outputs are shown in Fig. 7, which agree with the MATLAB outputs from the proposed chaotic system as shown in Fig. 1. These results confirm the physical feasibility of our proposed mathematical model.

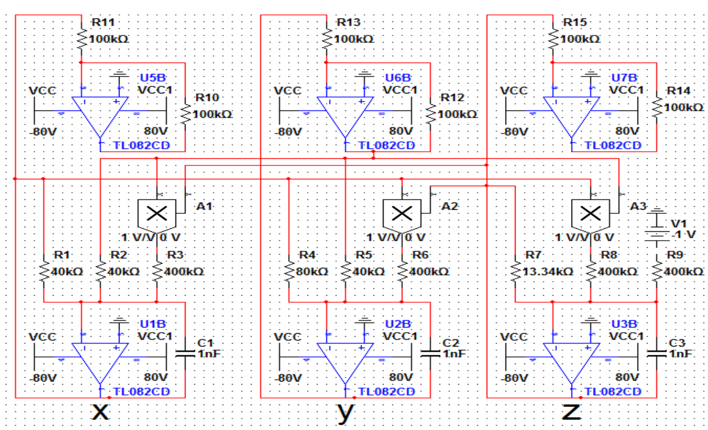

Fig. 6. The schematic circuit of the proposed chaotic system

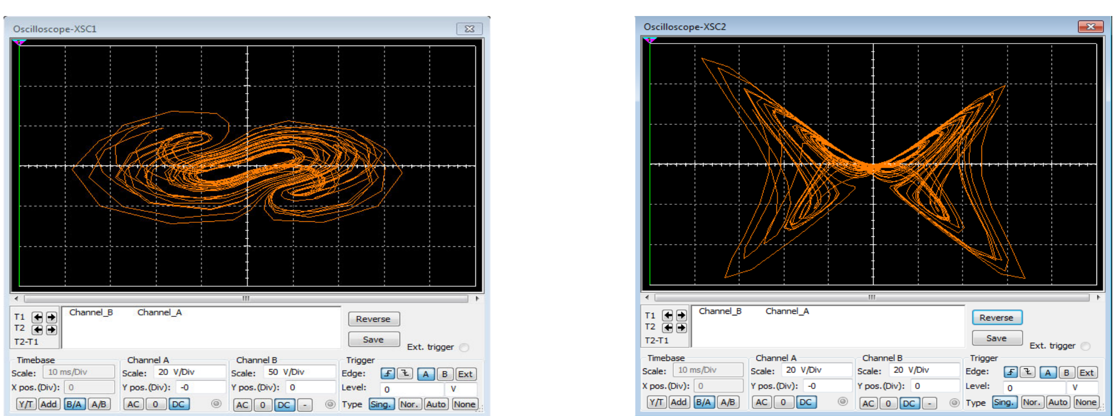

Fig. 7. Multisim outputs of the proposed chaotic system equivalent circuit

5. Pseudo Random Number Generator (PRNG) based on The Novel Four-Wing Chaotic System

The PRNG applications are one of the most frequently applied chaotic system applications (Kaçar, 2022a, 2022b; Aricioğlu & Kaçar, 2022). Testing the dynamic features of chaotic systems and their capacity to produce random numbers must be done to demonstrate the suitability of the suggested systems for applications. To do this, a new PRNG is created in this part based on the novel four-wing chaotic system as proposed. Fig. 8 shows the proposed PRNG's flowchart. As indicated in Fig. 8, the first step is identifying the system parameters, initials, and the number of bits to be extracted from the state variables throughout each iteration. The Runge-Kutta 4 (RK4) algorithm calculates state variables using the determined values. Each calculated state variable's float values are converted to binary form and XORed by taking the specified number of LSBs. In this case, the XOR operation is used to boost the unpredictability by analyzing all state variables' dynamic features. The test array receives the bits obtained from the XOR operation. When the test sequence reaches 1000000 bits, the widely used NIST-800-22 randomness test is used. This test suite consists of 15 tests, and for an array to be called random, it must select a value between the ranges of 1 and 0.001. As seen in Table 3, all PRNG results are good. Therefore, the newly proposed 3D chaotic system based PRNG has enough randomness. The processes are restarted, the input settings are updated, and a retry is done if even one of the tests fails.

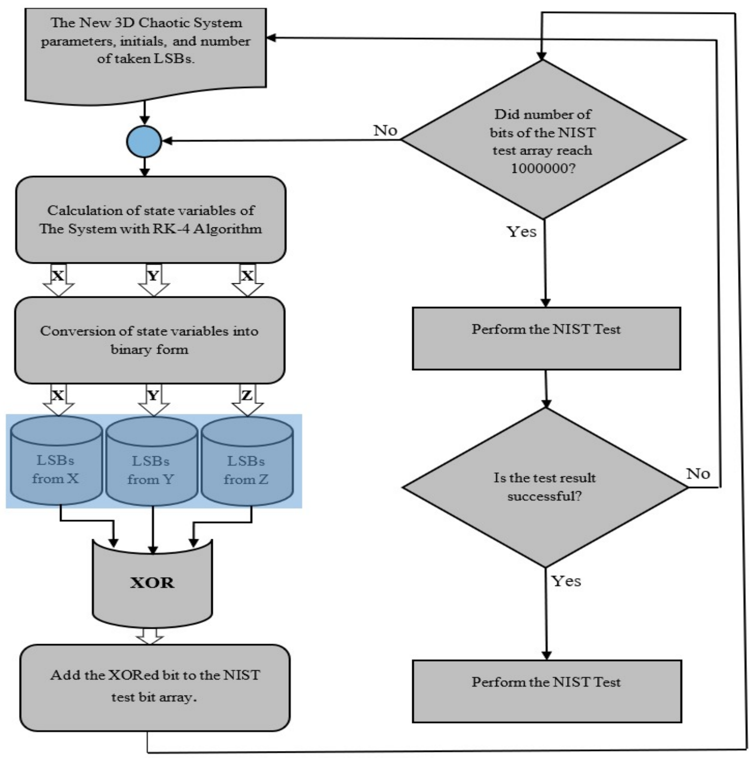

Fig. 8. Flowchart of PRNG

Table 3
NIST-800-22 based Randomness Test Result for the Proposed PRNG

Type of Statistical Tests	P-value (X)	P-value (Y)	P-value (Z)	Successful
Frequency (Monobit) Test	0.683273674902085	0.103949655360595	0.717352030441153	Success
Block-based Frequency Test	0.537732313521772	0.294231375008842	0.971201391987054	Success
Runs Test	0.82262774827221	0.474387848446585	0.101448988351208	Success
Block-based Longest-Run-of-Ones Test	0.625687611013713	0.175185662469405	0.452307942120757	Success
Binary Matrix Rank Test	0.90974977813845	0.326844488935768	0.523577533718785	Success
Discrete Fourier Transform Test	0.926883724880223	0.383328522648178	0.291282482860098	Success
Non-Overlapping Templates Matching Test	0.00533337860254232	0.00224062710749504	0.00327652637403605	Success
Overlapping Templates Matching Test	0.623102693699813	0.746830600474567	0.423452068200811	Success
Maurer's Universal Statistical Test	0.89972765146349	0.804486854436031	0.361037456900623	Success
Linear-Complexity Test	0.266230084303185	0.976222508833830	0.3518094600569680	Success
Serial Test-1	0.386150847527953	0.279397368962858	0.586760496317919	Success
Serial Test-2	0.279894949940472	0.104236698714838	0.491238129351486	Success
Approximate Entropy Test	0.690063721243611	0.130734761719028	0.31922694082635	Success
Cumulative-Sums Test	0.714868392443104	0.179014822495078	0.835015373918243	Success
Random-Excursions Test (x = -4)	0.308061639103337	0.822757924374886	0.194574681616521	Success
Random-Excursions Variant Test (x = -9)	0.0525765294646478	0.464988472593835	0.1692424400547	Success

6. PRNG Based Voice Encryption

PRNG-based voice encryption has been implemented in this part as a higher-level advanced application. The implemented application's encryption and decryption operations are shown in Fig. 9. The voice to be encrypted is initially provided as input for the encryption procedure. In this voice, values are changed from float to binary. On the other hand, the proposed 3D chaotic system's parameters and solution parameters are defined. Once more, the PRNG created in the previous section obtains the bit array by first obtaining the state variables with the RK4 technique. The XOR procedure is used to encrypt the binary bits from both the voice and the PRNG. A new set of voice values is obtained, and an encrypted voice is created by changing the encrypted bit array from binary to float. The encrypted voice is provided as input for the decryption process, and the bit array generated using the 3D chaotic system-based PRNG is also provided. Decrypted voice is obtained by converting encrypted voice values to binary form, then XORing them once more with a bit array taken from the PRNG.

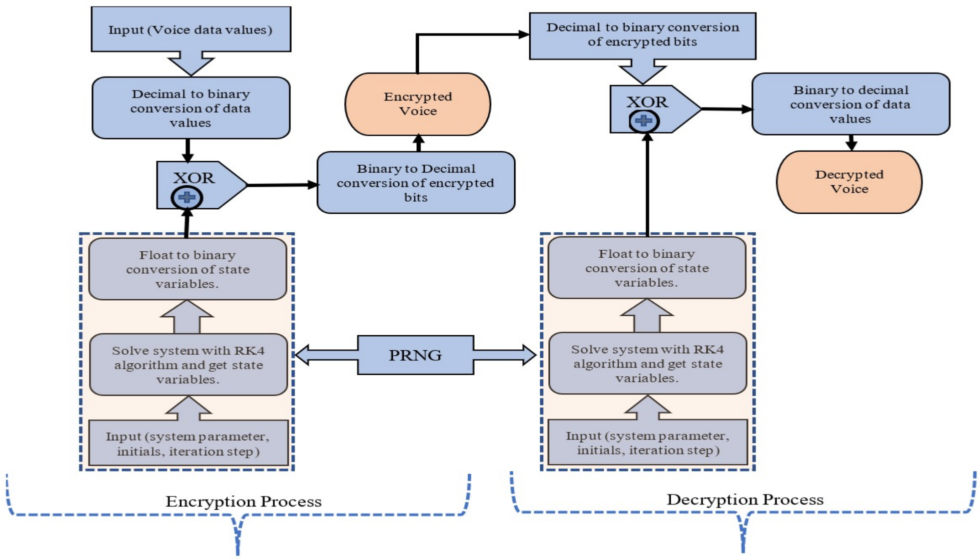

Fig. 9. Flowchart of encryption and decryption

To demonstrate the performance of the developed application, a speech-voice encryption process has been performed. The results are presented in Figs. 10 – 15 and Table 3. Fig. 10 and 11 show the used original voice and its frequency spectrum. Encrypted voice and its spectrum are presented in Figs. 12 and 13. Finally, Figs. 14 and 15 show the decrypted voice and its spectrum. When the figures of the original and encrypted voice are examined, it is observable that there is a complete difference in both the time and frequency domains. This indicates that the encryption process performs very well, and the original voice cannot be obtained with any filtering from the encrypted voice. When examining both figures, the original and the decrypted voice, we can observe that the same results were obtained in both the time and frequency domains. This shows that the original voice can be recovered without any losses of data during encryption and decryption processes.

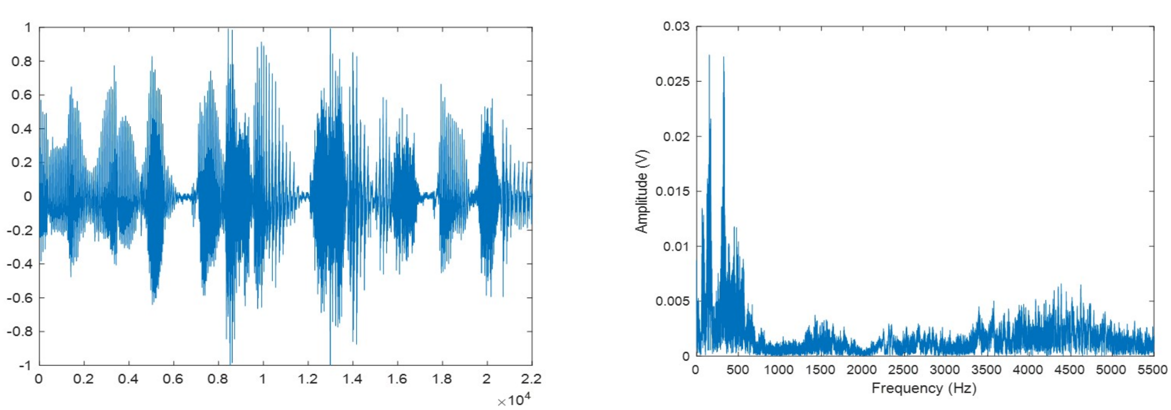

(a) (b)

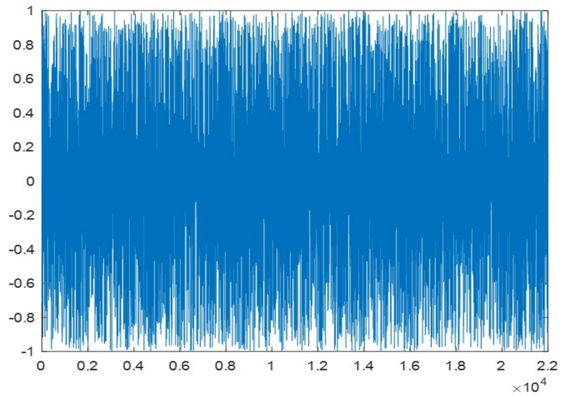

(c)

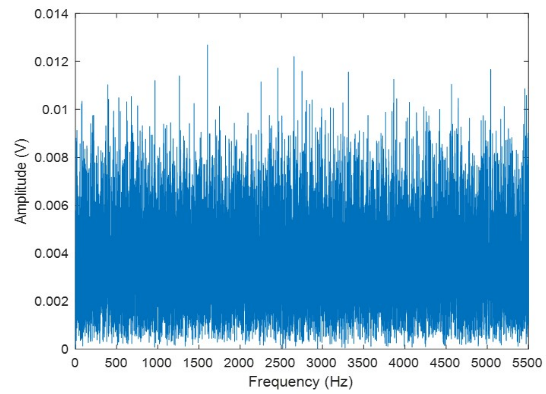

(d)

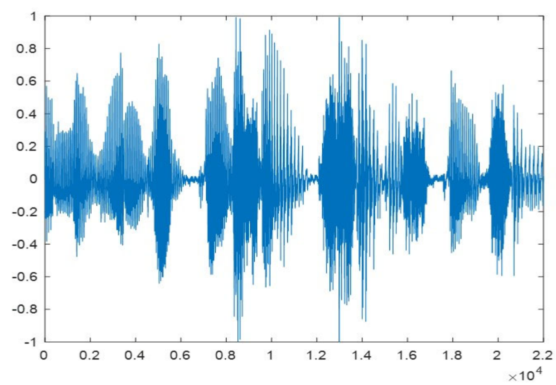

(e)

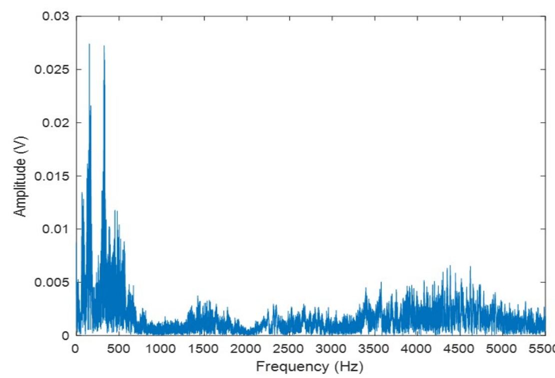

(f)

Fig. 10. The PRNG based on voice encryption results (a) original voice, (b) original voice spectrum, (c) encrypted voice, (d) encrypted voice spectrum, (e) decrypted voice and (f) decrypted voice spectrum.

Table 4
Statistical analysis results

	Original	**Encrypted**
Entropy	6.4669	14.4248
Correlation	0.5034	0.0101
PSNR	57.0095	
MSE	0.1295	
MAXERR	1.7529	
L2RAT	2.6062	

Table 4 captures the obtained results that were analyzed with entropy, correlation, peak signal-to-noise ratio (PSNR), mean square error (MSE), maximum squared error (MAXERR) and ratio of squared norms (L2RAT) methods. All the results in Table 2 prove that the implemented encryption application performs quite well. As a result, it has been seen that the new 3D chaotic system proposed in this study has sufficient dynamic and randomness features to be used for engineering applications.

7. Conclusions

In this work, we described a new model for another 3D multistable chaotic system with five-equilibrium and deduced that it had self-exited attractors. We showed that the proposed system could generate different coexisting attractors. In addition, we did a comparative study between our proposed system and other literature wherein we proved that the new system is much stronger than previously reported systems. We then examined the model's basic properties through bifurcation diagrams, maximum Lyapunov exponent, and phase portraits. We confirm its feasibility by utilizing Multisim software to construct the new chaotic system's electronic circuit. Finally, implementing the proposed voice encryption is done using a four-wing chaotic system based on the PRNG.

Acknowledgement

The authors are grateful to all reviewers for their comments and suggestions.

Funding Statement

The authors received no specific funding for this study.

Conflicts of Interest: All the authors declare that there is no conflict of interest.

References

Akmeşe, Ö. F. (2023). A Novel Random Number Generator and Its Application in Sound Encryption Based on a Fractional-Order Chaotic System. *Journal of Circuits, Systems and Computers*, *32*(03), 2350127.

Alemami, Y., Mohamed, M. A., Atiewi, S., & Mamat, M. (2020). Speech encryption by multiple chaotic maps with fast fourier transform. *International Journal of Electrical and Computer Engineering (IJECE)*, *10*(6), 5658-5664.

Al-Hazaimeh, O. M. (2020). A new dynamic speech encryption algorithm based on Lorenz chaotic map over internet protocol. *International Journal of Electrical and Computer Engineering (IJECE)*, *10*(5), 4824-4834.

Al-Hazaimeh, O. M., Abu-Ein, A. A., Nahar, K. M., & Al-Qasrawi, I. S. (2022). Chaotic elliptic map for speech encryption. *Indonesian Journal of Electrical Engineering and Computer Science*, *25*(2), 1103-1114.

Aricioğlu, B., & Kaçar, S. (2022). Circuit Implementation and PRNG Applications of Time Delayed Lorenz System. *Chaos Theory and Applications*, *4*(1), 4-9.

Benkouider, K., Bouden, T., Sambas, A., Mohamed, M. A., Sulaiman, I. M., Mamat, M., & Ibrahim, M. A. H. (2021). Dynamics, control and secure transmission electronic circuit implementation of a new 3D chaotic system in comparison with 50 reported systems. *IEEE Access*, *9*, 152150-152168.

Cai, G., & Tan, Z. (2007). Chaos synchronization of a new chaotic system via nonlinear control. *Journal of Uncertain systems*, *1*(3), 235-240.

Chen, Z., Yang, Y., & Yuan, Z. (2008). A single three-wing or four-wing chaotic attractor generated from a three-dimensional smooth quadratic autonomous system. *Chaos, Solitons & Fractals*, *38*(4), 1187-1196.

Cui, L., Lu, M., Ou, Q., Duan, H., & Luo, W. (2020). Analysis and circuit implementation of fractional order multi-wing hidden attractors. *Chaos, Solitons & Fractals*, *138*, 109894.

Deng, Q., Wang, C., & Yang, L. (2020). Four-wing hidden attractors with one stable equilibrium point. *International Journal of Bifurcation and Chaos*, *30*(06), 2050086.

Elsadany, A. A., Hussein, S., Al-khedhairi, A., & Elsonbaty, A. (2023). On dynamics of 4-D blinking chaotic system and voice encryption application. *Alexandria Engineering Journal*, *70*, 701-718.

Faradja, P., & Qi, G. (2020). Analysis of multistability, hidden chaos and transient chaos in brushless DC motor. *Chaos, Solitons & Fractals*, *132*, 109606.

Farsana, F. J., & Gopakumar, K. (2016). A novel approach for speech encryption: Zaslavsky map as pseudo random number generator. *Procedia computer science*, *93*, 816-823.

Gao, S., Wu, R., Wang, X., Wang, J., Li, Q., Wang, C., & Tang, X. (2023). A 3D model encryption scheme based on a cascaded chaotic system. *Signal Processing*, *202*, 108745.

García-Sepúlveda, O., Posadas-Castillo, C., Cortés-Preciado, A. D., Platas-Garza, M. A., Garza-González, E., & Sánchez, A. G. (2020). Synchronization of fractional-order Lü chaotic oscillators for voice encryption. *Revista mexicana de física*, *66*(3), 364-371.

Hassan, N. F., Al-Adhami, A., & Mahdi, M. S. (2022). Digital Speech Files Encryption based on Hénon and Gingerbread Chaotic Maps. *Iraqi Journal of Science*, 830-842.

Ilyas, B., Raouf, S. M., Abdelkader, S., Camel, T., Said, S., & Lei, H. (2022). An efficient and reliable chaos-based iot security core for udp/ip wireless communication. *IEEE Access*, *10*, 49625-49656.

Kaçar, S. (2022a). A new data-hiding algorithm for multi-channel biomedical signals based on variable-order fractional chaotic neural networks with frequency effect. *The European Physical Journal Special Topics*, *231*(5), 929-943.

Kaçar, S. (2022b). Digital circuit implementation and PRNG-based data security application of variable-order fractional Hopfield neural network under electromagnetic radiation using Grünwald-Letnikov method. *The European Physical Journal Special Topics*, *231*(10), 1969-1981.

Li, R. D. Y. (2014). Application of compound chaotic mapping in voice encryption algorithm. *International Journal of Computer Science and Network Security (IJCSNS)*, *14*(8), 44.

Liu, C., Liu, T., Liu, L., & Liu, K. (2004). A new chaotic attractor. *Chaos, Solitons & Fractals*, *22*(5), 1031-1038.

Lü, J., Chen, G., Cheng, D., & Celikovsky, S. (2002). Bridge the gap between the Lorenz system and the Chen system. *International Journal of Bifurcation and Chaos*, *12*(12), 2917-2926.

Mobayen, S., Volos, C., Çavuşoğlu, Ü., & S. Kaçar, S. (2020). A simple chaotic flow with hyperbolic sinusoidal function and its application to voice encryption. *Symmetry*, *12*(12), 2047.

Munmuangsaen, B., & Srisuchinwong, B. (2009). A new five-term simple chaotic attractor. *Physics Letters A*, *373*(44), 4038-4043.

Rahman, Z. A. S., & Jasim, B. H. (2022). Hidden Dynamics Investigation, Fast Adaptive Synchronization, and Chaos-Based Secure Communication Scheme of a New 3D Fractional-Order Chaotic System. *Inventions*, *7*(4), 108.

Rajagopal, K., Kacar, S., Wei, Z., Duraisamy, P., Kifle, T., & Karthikeyan, A. (2019). Dynamical investigation and chaotic associated behaviors of memristor Chua's circuit with a non-ideal voltage-controlled memristor and its application to voice encryption. *AEU-International Journal of Electronics and Communications*, *107*, 183-191.

Sadkhan, S. B., & Mohammed, R. S. (2015). Proposed random unified chaotic map as PRBG for voice encryption in wireless communication. *Procedia computer science*, *65*, 314-323.

Sambas, A., Vaidyanathan, S., Zhang, S., Zeng, Y., Mohamed, M. A., & Mamat, M. (2019). A new double-wing chaotic system with coexisting attractors and line equilibrium: bifurcation analysis and electronic circuit simulation. *IEEE Access*, *7*, 115454-115462.

Sambas, A., Vaidyanathan, S., Zhang, X., Koyuncu, I., Bonny, T., Tuna, M., ... & Kumam, P. (2022). A novel 3D chaotic system with line equilibrium: multistability, integral sliding mode control, electronic circuit, FPGA implementation and its image encryption. *IEEE Access, 10*, 68057-68074.

Vaidyanathan, S. (2016). Analysis, adaptive control and synchronization of a novel 4-D hyperchaotic hyperjerk system via backstepping control method. *Archives of Control Sciences*, *26*(3), 311-338.

Zhang, S., Zeng, Y., & Li, Z. (2018). One to four-wing chaotic attractors coined from a novel 3D fractional-order chaotic system with complex dynamics. *Chinese Journal of Physics*, *56*(3), 793-806.

Zhao, Y., Meng, R., Zhang, Y., & Yang, Q. (2023). Image encryption algorithm based on a new chaotic system with Rubik's cube transform and Brownian motion model. *Optik*, *273*, 170342.

Zhou, L., Wang, C., & Zhou, L. (2017). Generating four-wing hyperchaotic attractor and two-wing, three-wing, and four-wing chaotic attractors in 4D memristive system. *International Journal of Bifurcation and Chaos*, *27*(02), 1750027.